

Research Article

The Observation of Electrical Hysteric Behavior in Synthesized V_2O_5 Nanoplates by Recrystallization

Chang-Hee Kim,^{1,2} Yong Ju Yun,¹ Byung Hoon Kim,³ Won G. Hong,¹ Yark Yeon Kim,¹
Won Ick Jang,¹ Nae-Eung Lee,² and Han Young Yu¹

¹ Electronics and Telecommunications Research Institute (ETRI), 161 Gajeong-Dong, Yuseong-gu, Daejeon 305-700, Republic of Korea

² School of Advanced Materials Science and Engineering, Sungkyunkwan University, 300 Chunchun-Dong, Jangan-gu, Suwon, Kyunggi-do 440-746, Republic of Korea

³ Department of Physics, Incheon National University, Incheon 406-772, Republic of Korea

Correspondence should be addressed to Han Young Yu; uhan0@etri.re.kr

Received 2 May 2013; Accepted 24 July 2013

Academic Editor: Marcus C. Newton

Copyright © 2013 Chang-Hee Kim et al. This is an open access article distributed under the Creative Commons Attribution License, which permits unrestricted use, distribution, and reproduction in any medium, provided the original work is properly cited.

The anomalous electrical conductance for the V_2O_5 foam synthesized via a foaming process was measured. In the annealing process, the synthesized V_2O_5 foam is recrystallized with the increase of annealing temperature. The recrystallization procedure was characterized by using physical analysis tools such as thermogravimetric analysis (TGA), differential scanning calorimetry (DSC), scanning electron microscopy (SEM), high-resolution transmission electron microscopy (HRTEM), and X-ray diffractometer. In the electrical analysis technique of current-voltage characteristics as a function of annealing temperature, an anomalous hysteric behavior appears at the annealing temperature of 400°C. We conclude that the recrystallization of V_2O_5 nanoplates results in the anomalous behavior in voltage-dependent current characteristics.

1. Introduction

Vanadium oxide materials (VO_2 , V_2O_5 , and V_2O_3) [1–5] have been intensively studied in catalytic, electrochemical, and energy fields, such as an electrocatalyst for methanol oxidation [6], gas or biosensors [7, 8], cathode materials for lithium-ion batteries [9], and a hydrogen storage medium [10], due to their layered structure and high surface to volume ratio [11]. V_2O_5 materials exhibit various structures: nanowires, nanobelts, and macroporous structures according to their synthetic conditions [1, 12, 13].

The synthesis of crystalline V_2O_5 nanostructures for their various applications [7–10] has been actively investigated because of the unique properties of the crystalline nanostructures. The well-known synthetic techniques for single crystalline V_2O_5 nanostructures are hydrothermal treatments [11], electrochemical depositions [14], and vapor transports [15]. However, all these methods have several issues to overcome. Hydrothermal treatment needs to be performed at high

temperature and pressure. In electrodeposition technique, it demands long time to synthesize nanostructures using electrochemical equipment and chemical agents including toxic acid. The vapor transport technique should be accompanied by an electron beam evaporator operating in a high vacuum in order to fabricate V_2O_5 nanowires on silicon substrates.

Here, we present the simple and safe fabrication technique of a single crystalline V_2O_5 nanoplate using foaming processes and annealing routes [13, 16, 17] as well as the anomalous electrical conductance originated from the intermediate state of thermal annealing. The investigations for recrystallization of V_2O_5 form were done using physical analysis techniques such as TGA, DSC, SEM, HRTEM, and XRD as well as electrical properties of current-voltage characteristics. The anomalous behavior in current-voltage characteristics was measured at the annealing temperature of 400°C. With the correlation between structural and electrical analysis, we concluded that the anomalous behavior is related to the intermediate state of recrystallization.

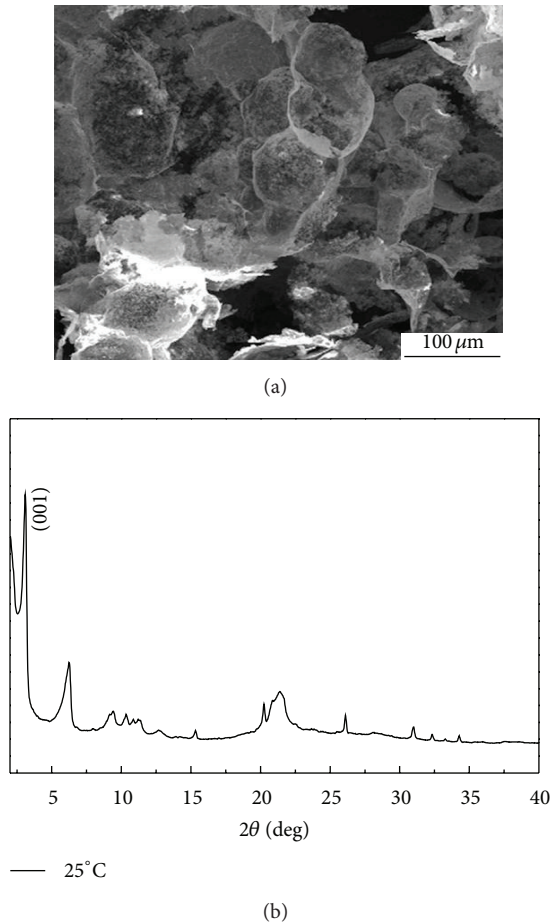


FIGURE 1: (a) SEM images and (b) XRD patterns of V_2O_5 foam dehydrated at room temperature.

2. Experimental

2.1. Materials and Synthesis. Macroporous V_2O_5 foams were synthesized by using the following procedures. (a) The yellow V_2O_5 gel was prepared from 1 g of commercial vanadium pentoxide (V_2O_5 , Aldrich) powder and 1.99 g of 1-hexadecylamine ($C_{16}H_{35}N$, Aldrich) in acetone (3 mL). (b) The formed gel was added in a concentrated H_2O_2 solution (50 mL, 30%). (c) After a few minutes, the gel spontaneously formed voluminous ultralight yellow foam by a decomposed oxygen gas from H_2O_2 . (d) The resultant foams were completely dehydrated at room temperature and then thermally annealed from 250°C to 600°C in air for 5 h.

2.2. Characterization. The morphology and size of the synthesized samples were studied by using a field emission scanning electron microscopy (FE-SEM, FEI Sirion 200) and a high-resolution transmission electron microscopy (HR-TEM, JEOL JEM-3010). The crystal structure of the samples was characterized by an X-ray diffractometer (XRD, Philips X'Pert) using graphite monochromatized $Cu K\alpha$ radiation

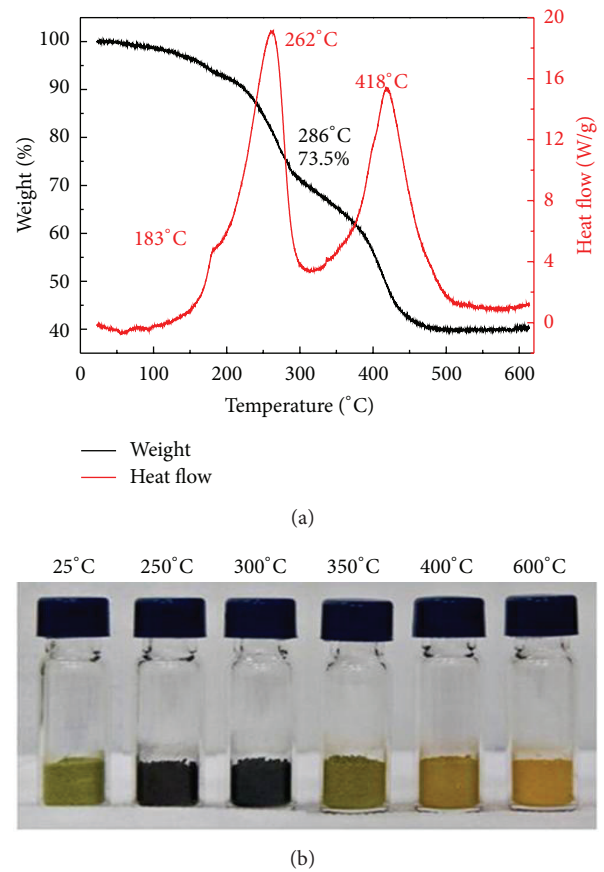


FIGURE 2: (a) Thermal analyses of V_2O_5 foam. (b) Optical image of V_2O_5 foam dehydrated room temperature and annealed from 250°C to 400°C.

($\lambda = 1.54178 \text{ \AA}$) and ratio K-Alpha2/K-Alpha1 of 0.5. Thermogravimetric analysis—differential scanning calorimeter (TGA and DSC, Setsys 16/18) was performed in a nitrogen gas environment with a heating rate of 3°C/min from 25°C to 600°C.

2.3. The Measurement of Electrical Properties. The electrical properties of V_2O_5 nanoplates were measured using Au/Ti (80 nm/20 nm) electrodes patterned onto SiO_2 substrate. The fabrication of the electrodes was done using I-line stepper (NSR2205i12D Stepper, Nikon, resolution: 0.35 μm) and E-beam evaporator with 1 μm width and pitch. In order to bridge the Au electrodes with V_2O_5 nanoplates, we adopted dielectrophoresis techniques. The applied peak-to-peak voltage and frequency in function generator are 10 V_{p-p} and 10 MHz, respectively. The suspension of V_2O_5 nanoplates in dehydrated ethanol was dropped (5 μL) onto the electrodes and ethanol was dried completely in air. The performance of anomalous behavior in terms of current-voltage characteristics was experimentally measured at room temperature for each of the nanoplates thermally annealed at different temperatures.

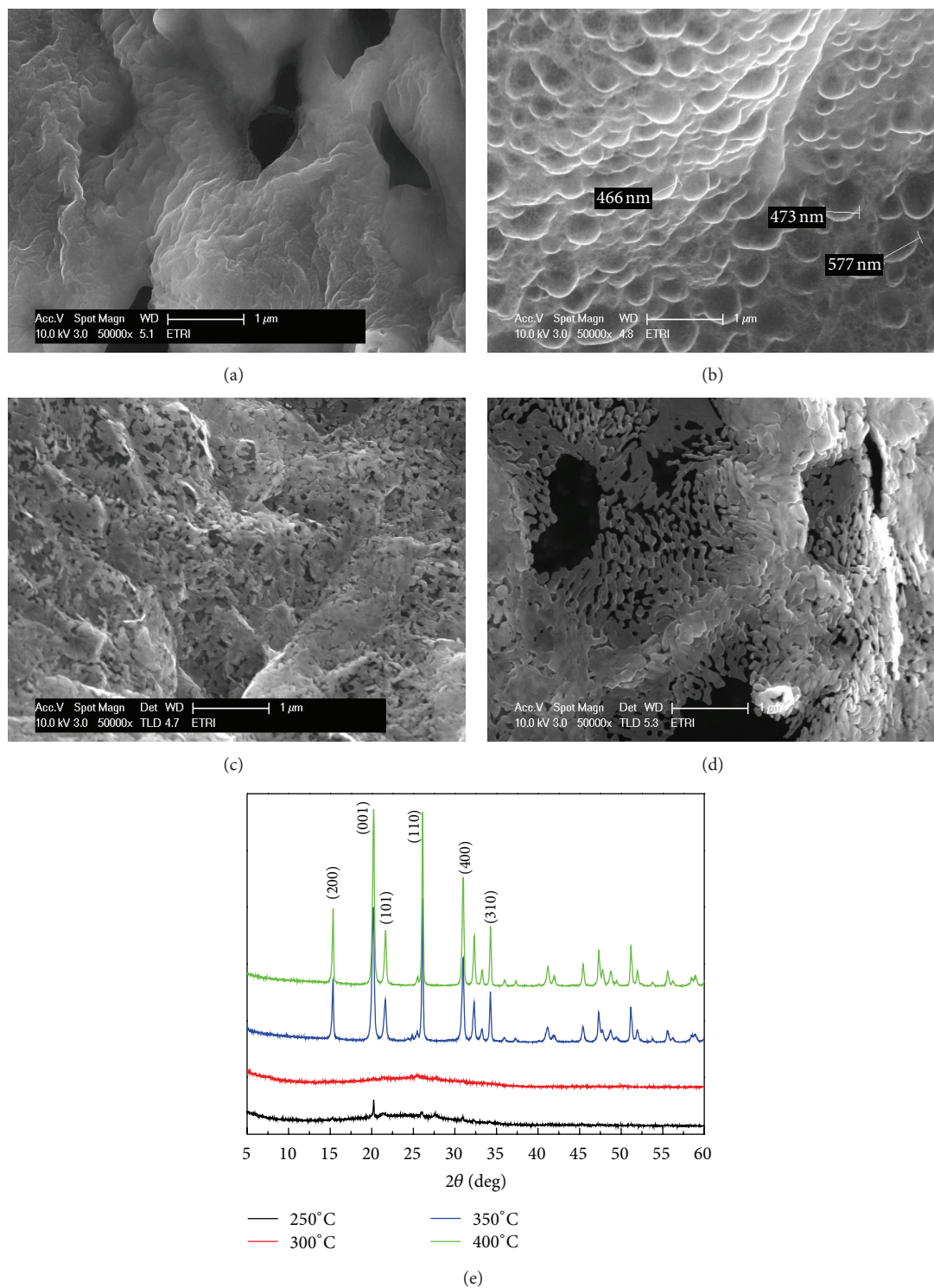


FIGURE 3: SEM image of V_2O_5 foam annealed at (a) 250°C, (b) 300°C, (c) 350°C, and (d) 400°C. (e) XRD patterns of V_2O_5 foam dependent on annealing temperature.

3. Results and Discussions

3.1. Morphology and Structure of V_2O_5 Foam. The morphology and crystallinity of the as-synthesized samples were studied from the images of an SEM and an XRD. Figure 1(a)

reveals that the dehydrated V_2O_5 foam at room temperature exhibits a macroporous, irregular, and grape-like morphology. In order to analyze the crystalline structure of dehydrated V_2O_5 foam, XRD analysis was followed. As shown in Figure 1(b), sharp peaks in XRD results appear at low angle,

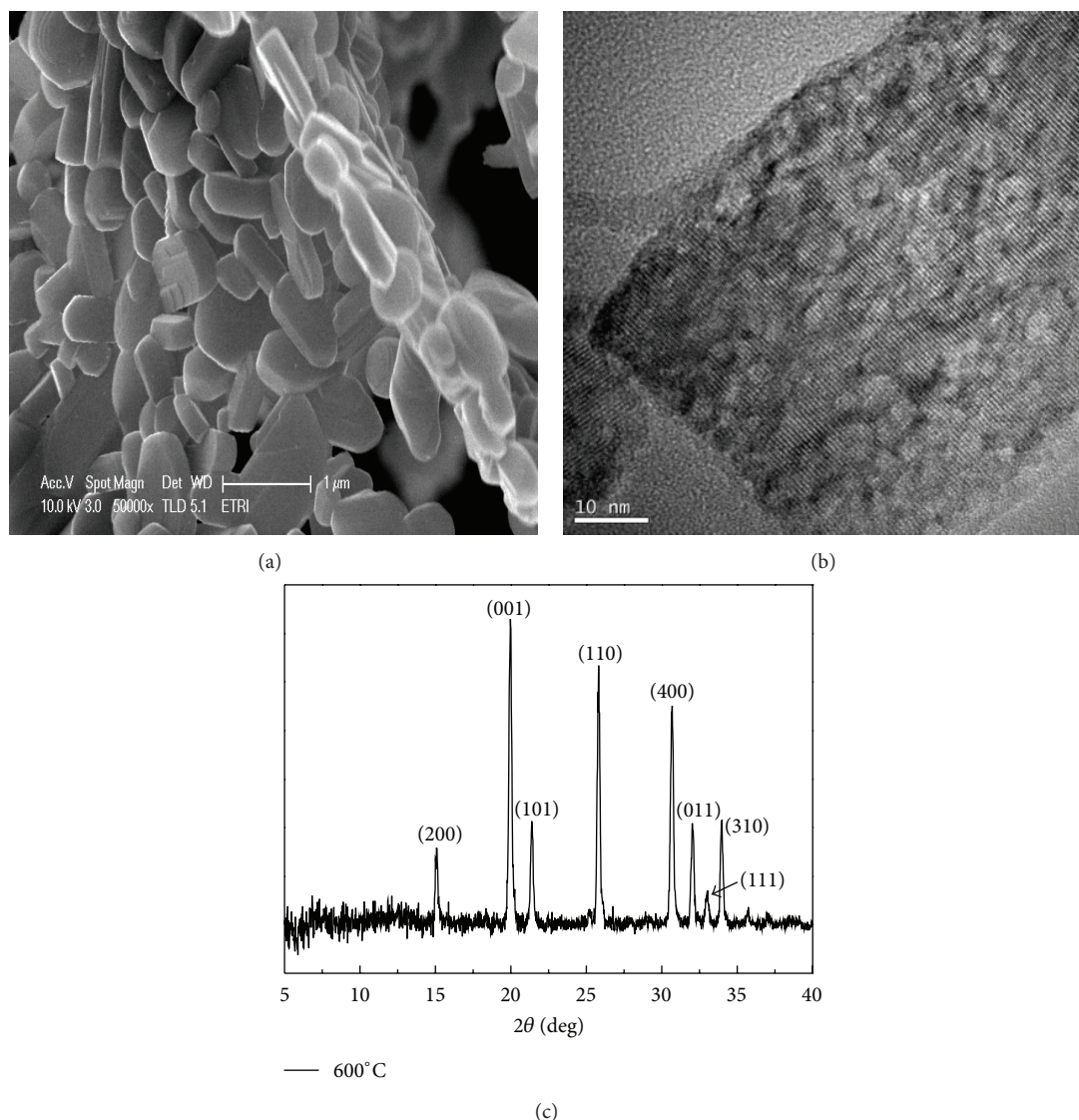


FIGURE 4: (a) SEM and (b) TEM image of V_2O_5 foam annealed at 600°C. (c) XRD patterns of V_2O_5 foam annealed at 600°C.

which can be assigned to the 001 peaks of lamellar solid [13]. From the first 001 peak, the interlayer distance was estimated as 28.5 Å, which is lower than that of hexadecylamine, 33.4 Å. The reduction of the interlayer distance is related to the adsorption of NH_3^{3+} onto vanadyl surface groups [18], which means that the creation of NH_3^{3+} by reaction of alkylamine ($-NH_2$) and H_2O_2 reduces the interlayer distance between the layers of vanadium oxide crystalline.

3.2. Thermal Analysis of V_2O_5 Foam. The thermal analysis for thermally annealed vanadium oxide form was performed using thermogravimetric analysis (TGA) and differential scanning calorimetry (DSC). The weight loss and heat flow as a function of increasing temperatures, respectively, related to the TGA and DSC can provide the information of physically oriented phase transition and chemically oriented decomposition. In the TGA and DSC results of the V_2O_5 foam as shown in Figure 2(a), three weight loss peaks appear relative to input temperatures, 183°C, 261°C, and 418°C. The first

peak corresponding weight loss of $\approx 6.4\%$ is related to the evaporation of the absorbed organic compounds on the foam surface, and the second peak corresponding weight loss of $\approx 23.6\%$ with an exothermic peak can be regarded as the decomposition of the hexadecylamine molecules intercalated among the V_2O_5 layers. The last weight loss ($\approx 30\%$) related to the third peak from 310°C to 420°C with an exothermic peak is originated from the recrystallization of the V_2O_5 foam. The colorimetric change of the annealed V_2O_5 as shown in Figure 2(b) also assists in the crystallization; with the increase of annealing temperature, the color of V_2O_5 foam changes from black to orange which means that recrystallization and related color of orange start from 310°C.

3.3. Morphology and Structure of Crystallized V_2O_5 Nanoplates. As was previously stated in Section 3.2, the recrystallization occurs above 310°C. However, a method of determining the structure of a crystal should be followed to confirm the crystallization such as SEM and XRD analyses.

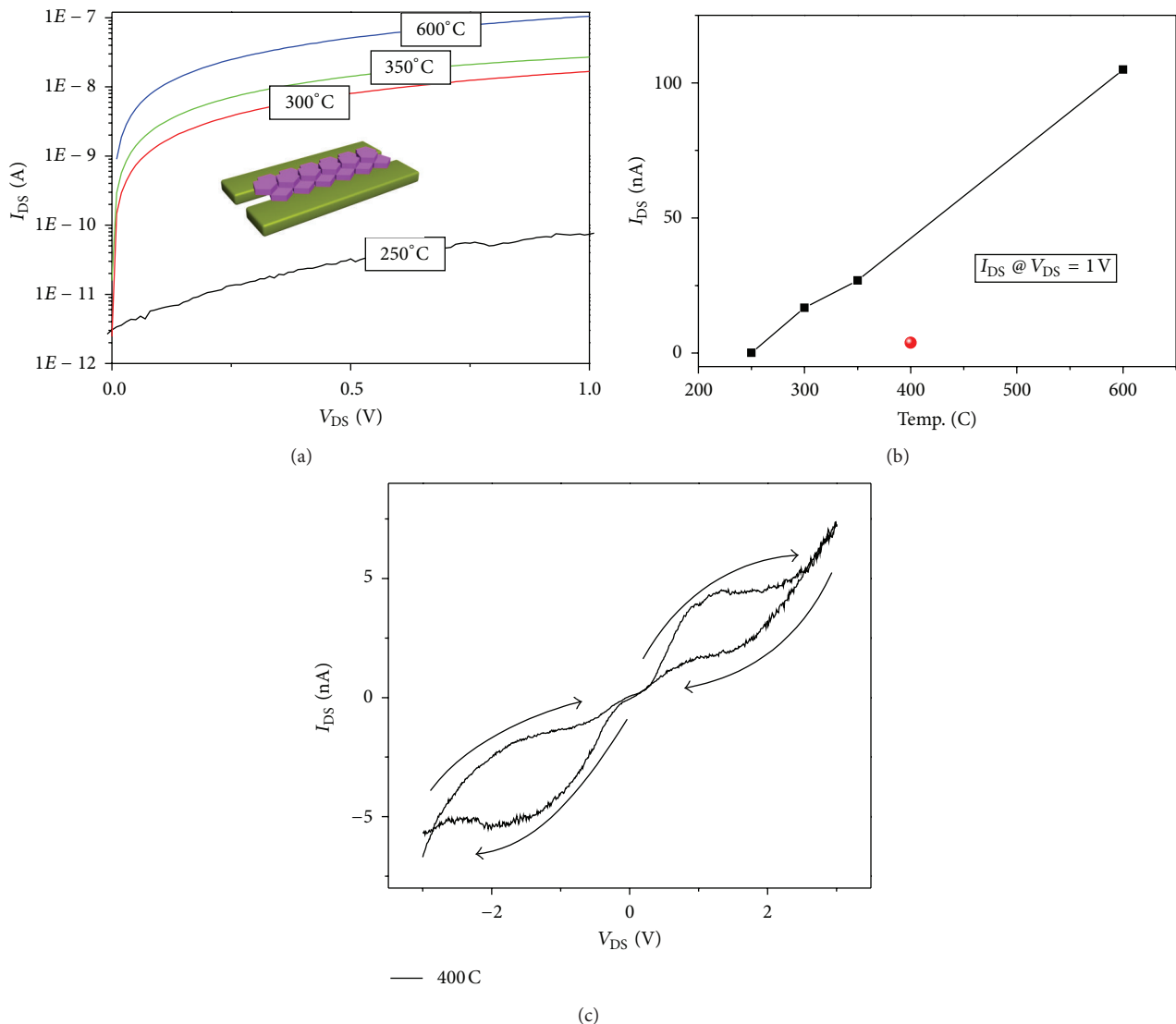


FIGURE 5: (a) Current-voltage characteristics of V_2O_5 nanoplates devices for different annealing temperatures from 250°C to 600°C except 400°C. Inset shows the schematic diagram of measured electronic devices V_2O_5 nanoplates and Au electrodes. (b) Plot of measured source-drain current as a function of temperature with fixed voltage of 1 V. (c) A current-voltage characteristic for the annealing temperature of 400°C.

The annealing temperature-dependent structural transition and crystallinity of the V_2O_5 results are demonstrated by SEM and XRD analyses as shown in Figure 3.

At annealing temperature of 250°C, the annealed V_2O_5 foam has a wrinkle-like morphology as shown in Figure 3(a). With the increase of annealing temperature up to 300°C, the embossed structure started to appear because of internal gas expansion inside the vanadium oxide as shown in Figure 3(b). When annealing temperature is higher than 310°C, the expanded embossing surface become to be open at annealing temperature of 350°C (Figure 3(c)). The opening of embossed at 350°C is related to the recrystallization mediated structural shrinkage, which is consistent with the third peak in TGA and DSC results above 310°C as well as the appearance of sharp peaks in XRD results at annealing temperature of 350°C (Figure 3(e)). The continuing recrystallization appears with

the increase of annealing temperature up to 400°C as shown in Figure 3(d). The embossed shape that appeared at 300°C disappeared clearly and plate-like structure is constructed, which means that the majority of V_2O_5 is considered to be recrystallized at annealing temperature of 400°C.

The recrystallization of V_2O_5 form also can be confirmed from the patterns of XRD. Figure 3(e) shows the XRD patterns of the crystal lattice transformation of the annealed samples at 250°C, 300°C, 350°C, and 400°C. The peaks in the XRD results are sharpened with the increase of annealing temperature. The amorphous structure at annealing temperature of 250°C and 300°C results in flattened XRD patterns and changes to be a crystallized orthorhombic structure above 350°C (JCPDS card no. 41-1426).

In order to validate the recrystallization procedures, the additional temperature annealing was performed up to 600°C

for 5 h. The recrystallization that started from 350°C is completely ended at annealing temperature of 600°C as shown in the SEM image of crystallized V₂O₅ nanoplate (Figure 4(a)). HRTEM image (Figure 4(b)) and XRD pattern (Figure 4(c)) also assist in the construction of an orthorhombic V₂O₅ single crystal with the basis distance of 4.38 Å.

3.4. Electrical Properties. The electrical properties of V₂O₅ form, the current-voltage characteristics, were measured with different annealing temperatures for the comparison of recrystallization in structural analysis. The current variations for the V₂O₅ nanoplates as a function of annealing temperature are depicted in Figure 5. In Figures 5(a) and 5(b), the current induced by applied source-drain voltage increases with the increase of annealing temperatures from 250°C to 600°C. At the annealing temperature of 400°C, however, the tendency of current-voltage characteristics (Figure 5(c)) and source-drain current as a function of annealing temperature with fixed voltage of 1 V shows hysteric and random behavior relative to that of the other temperatures, respectively.

The anomalous behavior in electrical characteristics is related to the recrystallization of V₂O₅ nanoplates including the possibilities for the presence of metal insulator transition [19, 20]. From the results of TGA, DSC, SEM, HRTEM, and XRD, the recrystallization started near the annealing temperature of 350°C and ended at 600°C. At annealing temperature of 400°C, however, an amorphous and a crystal structures coexist. Thus, we consider that the hysteric behavior at the annealing temperature of 400°C could be originated from the intermediated recrystallization of V₂O₅ nanoplates. The coexistence of crystal and amorphous structures makes it possible to make charge trap sites among the mixed states. As annealing temperature increases, the grain size of nanoplates increases. At critical temperature, however, the bubble foam shrinks quickly and it makes vacancy among nanoplates with the accompanying recrystallization of nanoplates (Figures 3(d) and 3(e)). The resulted mixed states appear as an anomalous conductance behavior as a function of annealing temperature and a hysteric current-voltage characteristic as shown in Figures 5(b) and 5(c), respectively.

4. Conclusions

We developed a simple synthetic technique for the crystallization of the V₂O₅ nanoplates from commercially provided irregular V₂O₅ powder. The synthetic technique is based on molecular assisted structural expansion, such as foaming construction. The annealing processes for the crystallization of V₂O₅ foam were done by using the routes of shrinkage of grain distance by thermal evaporation of the molecules. The crystallization procedure was confirmed via the thermal analysis tools of TGA and DSC and the structural analysis techniques of SEM, XRD, and TEM. In addition, we measured the electrical properties of synthesized and annealed V₂O₅ nanoplates. The electrical properties of the nanoplates show that the electrical conductance increased with the increase of annealing temperature from 250°C to 600°C except at 400°C where anomalous hysteric behavior appears. We consider that

the anomalous behavior is originated from the intermediated states of recrystallization, which was also confirmed from the correlations of thermal, structural, and electrical analysis.

Acknowledgments

This work was supported by the Ministry of Trade, Industry and Energy (no. 10043371) and Korea Research Council for Industrial Science and Technology.

References

- [1] J. Livage, "Vanadium pentoxide gels," *Chemistry of Materials*, vol. 3, no. 4, pp. 578–593, 1991.
- [2] W. Chen, J. Peng, L. Mai, Q. Zhu, and Q. Xu, "Synthesis of vanadium oxide nanotubes from V₂O₅ sols," *Materials Letters*, vol. 58, no. 17–18, pp. 2275–2278, 2004.
- [3] F. Sediri, F. Touati, and N. Gharbi, "From V₂O₅ foam to VO₂(B) nanoneedles," *Materials Science and Engineering B*, vol. 129, no. 1–3, pp. 251–255, 2006.
- [4] F. Sediri and N. Gharbi, "Controlled hydrothermal synthesis of VO₂(B) nanobelts," *Materials Letters*, vol. 63, no. 1, pp. 15–18, 2009.
- [5] J. Mendialdua, R. Casanova, and Y. Barbaux, "XPS studies of V₂O₅, V₆O₁₃, VO₂ and V₂O₃," *Journal of Electron Spectroscopy and Related Phenomena*, vol. 71, no. 3, pp. 249–261, 1995.
- [6] K.-F. Zhang, D.-J. Guo, X. Liu, J. Li, H.-L. Li, and Z.-X. Su, "Vanadium oxide nanotubes as the support of Pd catalysts for methanol oxidation in alkaline solution," *Journal of Power Sources*, vol. 162, no. 2, pp. 1077–1081, 2006.
- [7] H. Y. Yu, B. H. Kang, U. H. Pi, C. W. Park, S.-Y. Choi, and G. T. Kim, "V₂O₅ nanowire-based nanoelectronic devices for helium detection," *Applied Physics Letters*, vol. 86, no. 25, Article ID 253102, 3 pages, 2005.
- [8] V. Glezer and O. Lev, "Sol-gel vanadium pentoxide glucose biosensor," *Journal of the American Chemical Society*, vol. 115, no. 6, pp. 2533–2534, 1993.
- [9] A.-M. Cao, J.-S. Hu, H.-P. Liang, and L.-J. Wan, "Self-assembled vanadium pentoxide (V₂O₅) hollow microspheres from nanorods and their application in lithium-ion batteries," *Angewandte Chemie International Edition*, vol. 44, no. 28, pp. 4391–4395, 2005.
- [10] B. H. Kim, W. G. Hong, S. M. Lee et al., "Enhancement of hydrogen storage capacity in polyaniline-vanadium pentoxide nanocomposites," *International Journal of Hydrogen Energy*, vol. 35, no. 3, pp. 1300–1304, 2010.
- [11] S. Pavasupree, Y. Suzuki, A. Kitiyanan, S. Pivsa-Art, and S. Yoshikawa, "Synthesis and characterization of vanadium oxides nanorods," *Journal of Solid State Chemistry*, vol. 178, no. 6, pp. 2152–2158, 2005.
- [12] J. Ding, H. Peng, G. Li, and K. Chen, "Conversion of V₂O₅ · xH₂O into orthorhombic V₂O₅ single-crystalline nanobelts," *Materials Letters*, vol. 64, no. 14, pp. 1562–1565, 2010.
- [13] G. T. Chandrappa, N. Steunou, and J. Livage, "Materials chemistry: macroporous crystalline vanadium oxide foam," *Nature*, vol. 416, no. 6882, p. 702, 2002.
- [14] K. Takahashi, S. J. Limmer, Y. Wang, and G. Cao, "Synthesis and electrochemical properties of single-crystal V₂O₅ nanorod arrays by template-based electrodeposition," *Journal of Physical Chemistry B*, vol. 108, no. 28, pp. 9795–9800, 2004.

- [15] J. M. Velazquez and S. Banerjee, "Catalytic growth of single-crystalline V_2O_5 nanowire arrays," *Small*, vol. 5, no. 9, pp. 1025–1029, 2009.
- [16] Y. C. Hong and H. S. Uhm, "Crystalline vanadium nitride foam," *Scripta Materialia*, vol. 59, no. 2, pp. 262–264, 2008.
- [17] I. M. Arabatzis and P. Falaras, "Synthesis of porous nanocrystalline TiO_2 foam," *Nano Letters*, vol. 3, no. 2, pp. 249–251, 2003.
- [18] F. Carn, N. Steunou, J. Livage, A. Colin, and R. Backov, "Tailor-made macroporous vanadium oxide foams," *Chemistry of Materials*, vol. 17, no. 3, pp. 644–649, 2005.
- [19] H.-T. Kim, B.-G. Chae, D.-H. Youn et al., "Mechanism and observation of Mott transition in VO_2 -based two- and three-terminal devices," *New Journal of Physics*, vol. 6, no. 52, 2004.
- [20] M. Kang, I. Kim, S. W. Kim, J.-W. Ryu, and H. Y. Park, "Metal-insulator transition without structural phase transition in V_2O_5 film," *Applied Physics Letters*, vol. 98, no. 13, Article ID 131907, 3 pages, 2011.



Hindawi

Submit your manuscripts at
<http://www.hindawi.com>

